

See discussions, stats, and author profiles for this publication at: <https://www.researchgate.net/publication/44653730>

# Fluorescent Mannose-Functionalized Hyperbranched Poly(amido amine)s: Synthesis and Interaction with E. coli

ARTICLE in BIOMACROMOLECULES · JULY 2010

Impact Factor: 5.75 · DOI: 10.1021/bm100307d · Source: PubMed

---

CITATIONS

35

---

READS

43

## 4 AUTHORS, INCLUDING:



Wen Yang

Hefei University of Technology

5 PUBLICATIONS 99 CITATIONS

SEE PROFILE



Cai-Yuan Pan

University of Science and Technology of C...

108 PUBLICATIONS 3,579 CITATIONS

SEE PROFILE



Mingdeng Luo

Monash University (Australia)

3 PUBLICATIONS 43 CITATIONS

SEE PROFILE

# Fluorescent Mannose-Functionalized Hyperbranched Poly(amido amine)s: Synthesis and Interaction with *E. coli*

Wen Yang,<sup>†,‡</sup> Cai-Yuan Pan,<sup>\*,†</sup> Ming-Deng Luo,<sup>‡</sup> and Hong-Bin Zhang<sup>‡</sup>

Department of Polymer Science and Engineering, CAS Key Laboratory of Soft Matter Chemistry, University of Science and Technology of China, Hefei, Anhui 230026, People's Republic of China, and Department of Polymer Science and Engineering, Anhui Key Laboratory of Controllable Chemistry Reaction and Material Chemical Engineering, Hefei University of Technology, Hefei, Anhui 230009, People's Republic of China

Received March 22, 2010; Revised Manuscript Received May 13, 2010

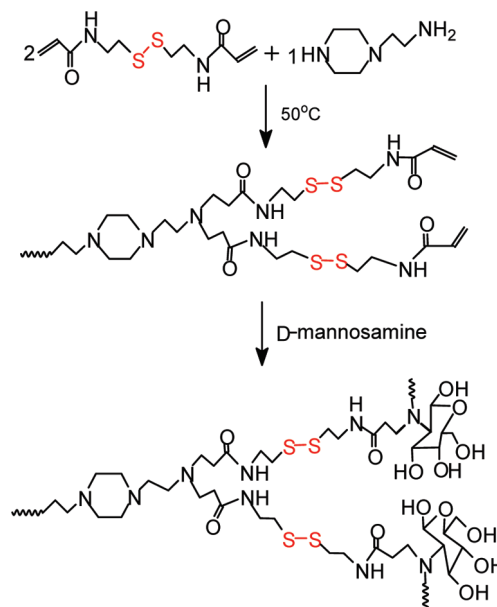
A water-soluble, biodegradable and fluorescent hyperbranched poly(amidoamine) with mannose groups on their surface (M-HPAMAM) has been successfully prepared, and the synthetic strategy includes Michael addition polymerization of diacrylamide with 1-(2-aminoethyl)piperazine and, subsequently, surface modification with mannosamine. The photoluminescence of M-HPAMAM was enhanced significantly due to the surface mannose groups. Incubation of *E. coli* with M-HPAMAMs yielded brightly fluorescent bacteria clusters, but the fluorescent intensity of the aqueous solution lowered. This indicates that the M-HPAMAMs have strong affinity with bacteria due to their polyvalent interactions. Based on the size and the amount of bacteria clusters formed, the bacteria with the concentrations higher than  $10^2$  cfu/mL can be detected.

## Introduction

Poly(amido amine)s (PAMAMs) are well-known biocompatible polymers and have been extensively studied for use as biomedical materials and polymer therapeutics.<sup>1–5</sup> As one of the most promising biodegradable polymers, PAMAMs were applied in the preparation of safe and efficient nonviral gene vectors due to their low cytotoxicity and high transfection efficiency.<sup>6–8</sup> The modified PAMAM dendrimers were pH-sensitive and can be used as efficient anticancer drug carriers.<sup>9–11</sup> In testing their functions in vitro or in vivo, addition of the fluorescent labels onto the PAMAMs is often required. However, this needs multiple steps and may result in a decrease in the biocompatibility. If the polymers can emit strong fluorescence, the labeling procedure can be omitted.

In an investigation on the synthesis and properties of the hyperbranched PAMAMs (HPAMAMs), we observed the fluorescence of such polymers, but photoluminescence was not so strong.<sup>12</sup> A similar phenomenon was also observed by other research groups.<sup>13,14</sup> We found that the tertiary amine in the HPAMAMs is a key unit for the fluorescence property because the fluorescence was quenched when the tertiary amine groups in the HPAMAMs were quaternized by  $\text{CH}_3\text{I}$ .<sup>12</sup> The linear PAMAM containing only the primary and secondary amines did not display fluorescent property.<sup>12</sup> These results were supported by early investigation of the tertiary amine compounds. Generally triethyl amine in solution can not emit fluorescence, but trimethylamine, triethylamine, and tri(*n*-propyl)amine in the gas phase emitted strong fluorescence, owing to a significant decrease in the collisional relaxation rate, and for the primary amines and secondary amines, no fluorescence was observed even if they were in gas phase because of their high predissociation rate.<sup>15,16</sup> These results imply that the hyperbranched structure has the function of reducing the

**Scheme 1.** Synthetic Process of Mannose-Functionalized Hyperbranched Poly(amido amine)s



collisional relaxation rate similar to the function of the tertiary amines in the gas phase. So, enhancing the fluorescence of HPAMAM can be achieved by increasing the content of the tertiary amine units and adjusting the branched structures. The biocompatible and biodegradable polymers with autofluorescence should have broad applications in various fields.

For detection of bacteria, traditional methods such as plating and culturing are time-consuming (generally several days).<sup>17,18</sup> Facile methods for rapid and efficient detection of bacteria are based on the fluorescent intensity changes of the samples. Most of the detecting reagents reported are dye-doped nanoparticles, such as silica,<sup>19</sup> gold,<sup>20</sup> and magnetic nanoparticles,<sup>21,22</sup> with their surface having bacteria affinitive groups or biomolecules, such as antibodies<sup>19</sup> or carbohydrate.<sup>23</sup> So, the reagents capable

\* To whom correspondence should be addressed. Fax: (+86)551-3601590. E-mail: pcy@ustc.edu.cn.

<sup>†</sup> University of Science and Technology of China.

<sup>‡</sup> Hefei University of Technology.

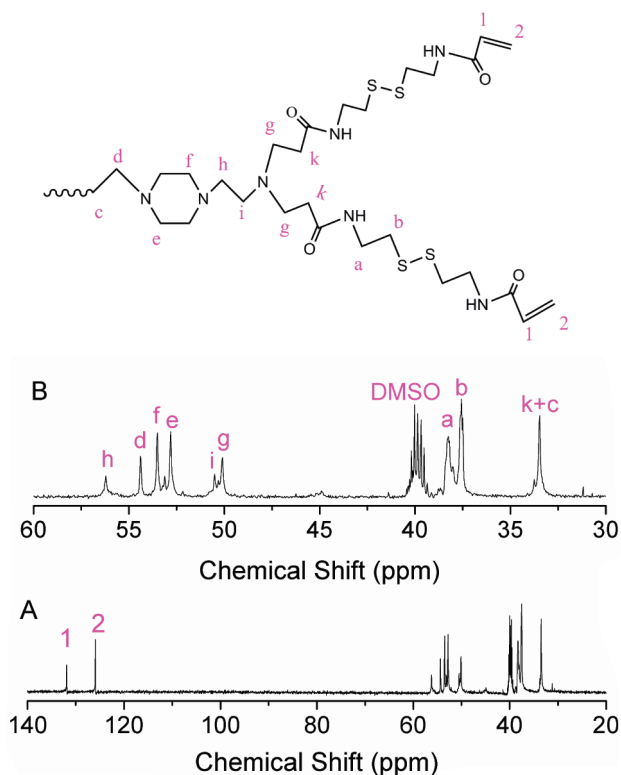


**Figure 1.**  $^{13}\text{C}$  NMR spectra of the hyperbranched PAMAMs in  $\text{DMSO}-d_6$ ; B is part of A from 30 to 60 ppm. Preparation conditions of HPAMAMs: feed molar ratio, CBA/AEPZ = 2/1; 50 °C; 5 days.

of bacteria detection should have two functions: the strong affinity with bacteria and the bright photoluminescence.

Generally, the individual carbohydrate–protein interactions are weak, but such interactions can be strengthened via cooperative multiple interactions.<sup>24</sup> For example, the fluorescent conjugated polymers or columnar supramolecular polymers with pendant sugar residues exhibited strong interaction with the bacteria.<sup>25–27</sup> However, the polymers containing conjugated phenyl units are not degradable and have potential carcinogenesis or toxicity, and the fluorescent organic dyes used in doped-nanoparticles, which are often conjugated aromatic compounds, exhibit poor photostability and substantial cytotoxicity.<sup>28</sup> Thus, the development of a water-soluble, biocompatible, and biodegradable HPAMAM with multiple functionalities including strong fluorescence and strong affinity to bacteria is of crucial demand. Because disulfide linkages can easily cleave in the presence of biological or chemical stimuli,<sup>3,29</sup> the HPAMAMs containing disulfide linkages are prepared via Michael addition polymerization of *N,N'*-cystaminebisacrylamide (CBA) and 1-(2-aminoethyl) piperazine (AEPZ). Mannose displayed strong interaction with bacteria<sup>23</sup> and also may enhance the fluorescence of the resulting polymer, therefore, the surface modification of the resultant HPAMAMs with mannosamine is performed. Thus, the purpose of this article is the synthesis of mannosamine-functionalized HPAMAMs containing disulfide linkages in their backbone and investigation of their functions: strong fluorescence and the specific affinity to bacteria.

### Experimental Section

**Materials.** Cystamine dihydrochloride ( $\geq 98\%$ , Changzhou Furong Chemical Co.), 1-(2-aminoethyl) piperazine (AEPZ, 99%, Aldrich), D-mannosamine hydrochloride ( $\geq 98.5\%$ , Shanghai Yuanju Biochemical Company), dichloromethane ( $\geq 99.5\%$ ), methanol ( $\geq 99.5\%$ ), and

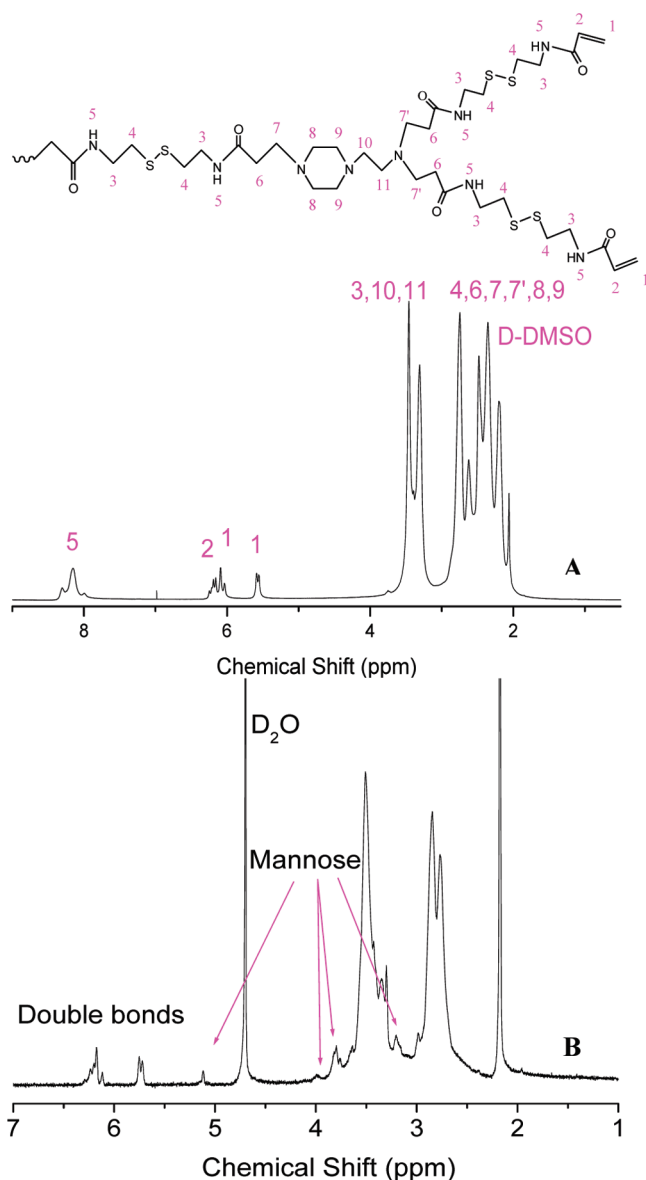


**Figure 2.**  $^1\text{H}$  NMR spectra of the hyperbranched PAMAMs (A) in  $\text{DMSO}-d_6$  and the mannose-functionalized hyperbranched PAMAMs (B) in  $\text{D}_2\text{O}$ . Preparation conditions of HPAMAMs: feed molar ratio, CBA/AEPZ = 2/1; 50 °C; 5 days.

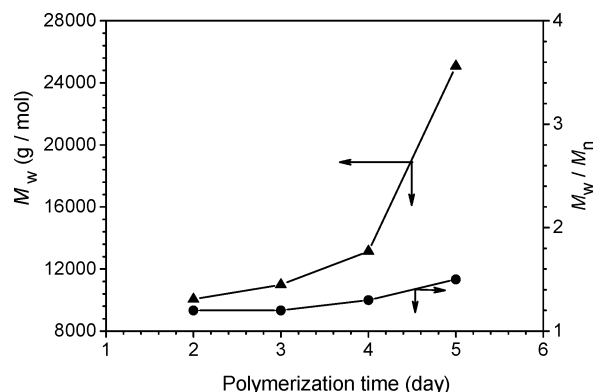


**Figure 3.** Relationship of  $M_w$  and  $M_w/M_n$  with polymerization time. Polymerization conditions: feed molar ratio of CBA/AEPZ, 2/1; solvent, 2 mL of methanol/water mixture (85/15, v/v); 50 °C.

acetone ( $\geq 99.5\%$ ) were purchased from Sinopharm Chemical Reagent Co. and used as received. Acryloyl chloride was purified by distillation under reduced pressure.

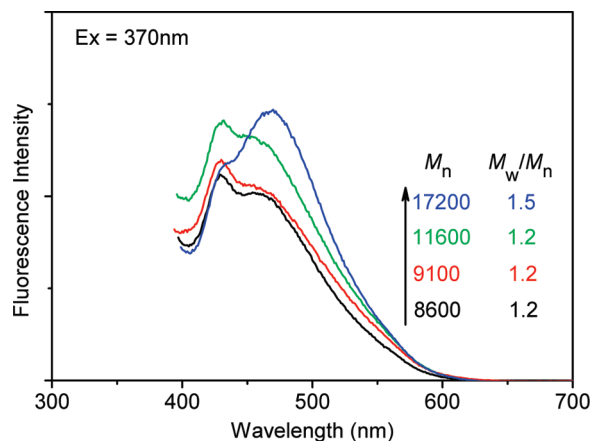


**Figure 4.** Fluorescent spectra of HPAMAMs with different molecular weights obtained, respectively, from 2, 3, 4, and 5 days of polymerization in methanol/water (85/15, v/v),  $\lambda_{\text{ex}} = 370$  nm. Polymerization conditions: feed molar ratio of CBA/AEPZ, 2/1; 50 °C.

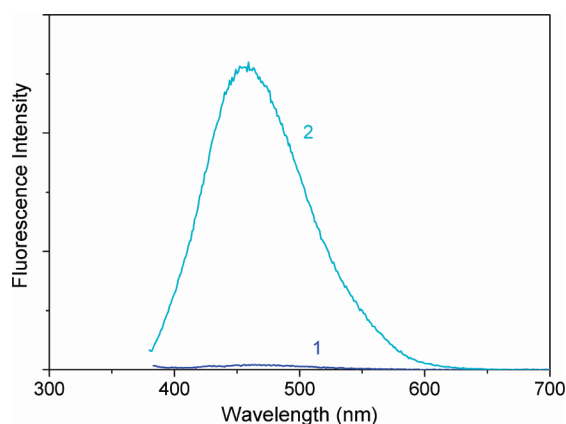


**Figure 5.** Fluorescent spectra of HPAMAMs formed at 5 days of polymerization in the methanol/water mixture (85/15, v/v; 1) and then modified with mannosamine (2). Concentration for fluorescence measurement, 1 mg/mL; room temperature;  $\lambda_{\text{ex}} = 370$  nm. Polymerization conditions: feed molar ratio of CBA/AEPZ, 2/1; 50 °C.

**Characterizations.**  $^1\text{H}$  NMR measurements were performed on a Bruker DMX-300 spectrometer using  $\text{D}_2\text{O}$  or  $\text{DMSO}-d_6$  as solvent. The weight- ( $M_w$ ) and number-average molecular weight ( $M_n$ ) and polydispersity index of the polymers were determined on a Waters gel permeation chromatography (GPC) at 50 °C using two Styragel columns, HT3 and HT4 in series. A Waters 1515 pump and Waters 2414 differential refractive index detector (set at 35 °C) were used. DMF was used as eluent at a flow rate of 1.0 mL/min. A series of six low polydispersity polystyrene standards with molecular weights ranging from 800 to 400000 g/mol were used for the calibration of molecular weights. The measurement of fluorescence spectra was carried out at room temperature on a Shimadzu RF-5301PC luminescence spectrophotometer. Phase contrast and fluorescence microscopy images were performed on an Olympus IX70 microscope with three kinds of filters (WU: 330–385 nm, WB: 460–490 nm, and WG: 510–550 nm). Laser confocal fluorescence microscopy was performed on a Carl Zeiss LSM 510. Transmission electron microscopy (TEM) images were obtained on JEOL 2010 electron microscopes operated at 200 kV.

**Synthesis of  $N,N'$ -Cystaminebisacrylamide (CBA).** Cystamine dihydrochloride (5.8 g, 25 mmol) was added into 60 mL of aqueous NaOH (4 g, 100 mmol) solution in a three-necked round-bottom flask. A solution of acryloyl chloride (4.7 g, 50 mmol) in dichloromethane (5 mL) was added dropwise while stirring at 0 °C. After the addition was complete, the mixture was stirred at room temperature for 3 h. The solid product was obtained by filtration. The liquid phase was extracted with dichloromethane, and the organic extract was dried over

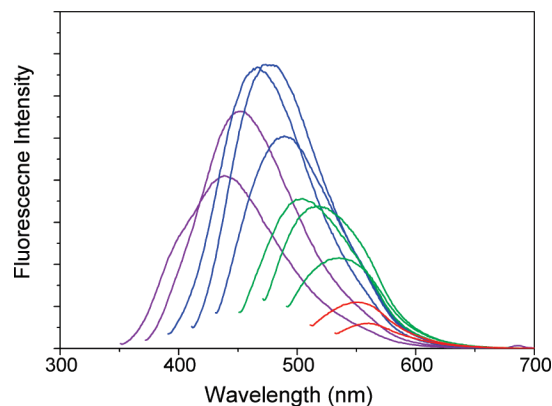


**Figure 6.** Fluorescence spectra of the M-HPAMAMs solution in water (0.2 wt %) with progressively longer excitation wavelengths, from 340 nm on the left to 520 nm on the right, in 20 nm increments.

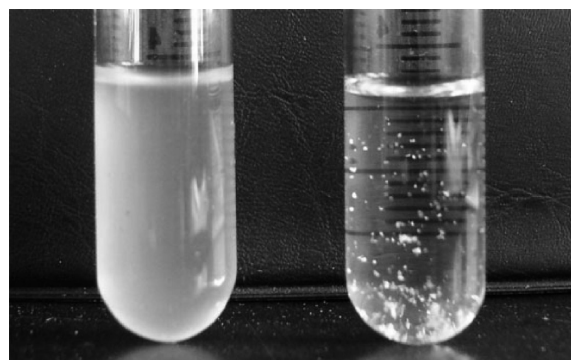


**Figure 7.** Optical images of *E. coli* at OD1.0 (left) and *E. coli* at OD1.0 incubated with M-HPAMAMs (right).

anhydrous  $\text{Na}_2\text{SO}_4$  overnight. The solvent was removed under reduced pressure. The final product was obtained as a white solid (4.2 g, 65%).  $^1\text{H}$  NMR (300 MHz,  $\text{CDCl}_3$ ,  $\delta$ , TMS): 6.57 (2H, -CONH-), 6.36 and 6.22 (4H,  $\text{CHH}=\text{CHCO}-$ ), 5.69 (2H,  $\text{CHH}=\text{CHCO}-$ ), 3.67 (4H, -CONHCH $_2$ CH $_2$ SS-), 2.89 (4H, -CONHCH $_2$ CH $_2$ S-).  $^{13}\text{C}$  NMR (300 MHz,  $\text{CDCl}_3$ ,  $\delta$ , TMS): 167 (-CONHCH $_2$ -), 131 ( $\text{CH}_2=\text{CH}-$ ), 126 ( $\text{CH}_2=\text{CH}-$ ), 39 (-CONHCH $_2$ CH $_2$ SS-), 38 (-CONHCH $_2$ CH $_2$ SS-).

**Synthesis of Mannose-Functionalized Hyperbranched Poly(amido amine)s.** The CBA (0.26 g, 1 mmol) and AEPZ (0.065 g, 0.5 mmol) were added into a 2 mL methanol/water mixture (85/15, v/v), and the polymerization was carried out at 50 °C for 5 days. Then the polymerization mixture was precipitated in cool acetone, and the solid was collected by filtration and then dried in a vacuum oven for molecular weight measurement. Molecular weight of the HPAMAM was measured by GPC method ( $M_n = 17500$ , PDI = 1.42).

D-Mannosamine hydrochloride (0.216 g 1 mmol) was added into the reaction solution; after the addition was complete, the reaction mixture was stirred for 2 days. The solution was acidified with 2 N HCl aqueous solution until pH  $\sim$  2. Then the solution was added into 30 mL of cool acetone while vigorously stirring. The polymer was collected by filtration and then purified by reprecipitation in cool acetone. The product was dried in vacuum for 1 day at room temperature.

***E. coli* Detection.** *Escherichia coli* (*E. coli*) BL21 was used in the detection studies. *E. coli* cells were grown in LB media at 37 °C until they reached an approximate  $10^9$  cfu/mL (plate-counting method). The bacteria solution was collected in Eppendorf tubes and centrifuged at 10000 g for 30 min at 4 °C. Sterile phosphate-buffered saline (PBS, pH = 7.2, 0.01 M phosphate, 0.5 M NaCl,  $0.1 \times 10^{-3}$  M  $\text{MnCl}_2$ , and  $0.1 \times 10^{-3}$  M  $\text{CaCl}_2$ ) solution was used to wash *E. coli* cells three times. The various concentrations of *E. coli* cells were achieved through serial 10-fold dilutions.



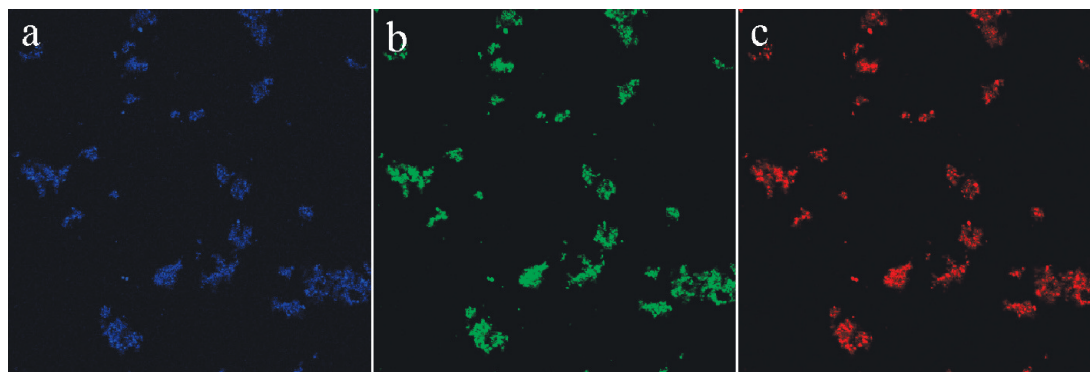


**Figure 8.** Laser confocal fluorescence microscopy images of *E. coli* strain BL21 at OD1.0 with M-HPAMAMs at an excitation wavelength of 800 (a), 488 (b), and 543 nm (c).

Aqueous solution of the polymer (50  $\mu$ L, 10 mg/mL) was added to a 4 mL PBS solution of *E. coli* cells with OD 1.0. The suspension was then incubated for 20 min at room temperature with gentle shaking, and lots of aggregates were formed. The suspension was centrifuged at 10000 g for 10 min, and the aggregates obtained were washed three times with PBS solution and redispersed in the 4 mL PBS solution.

### Results and Discussion

**Synthesis of Mannose-Functionalized HPAMAM.** It is well-known that the disulfide bond is readily cleavable under chemical and biological stimuli such as dithiothreitol, tributylphosphine, 2-mercaptoethanol, and glutathione under mild conditions.<sup>3,28,29</sup> So, the HPAMAMs with disulfide groups in their backbone were prepared by Michael addition polymerization of AEPZ and CBA. The synthetic procedure is shown in Scheme 1. We tried to modify the surface of HPAMAMs with mannosamine for enhancing the fluorescence and the interactions with objects. As we mentioned in the Introduction, an increase in the tertiary amine groups and regulation of the hyperbranched structure can improve the fluorescence. The mannosamine was selected as a modifier because (1) the mannose displayed strong interaction with bacteria;<sup>23</sup> (2) more tertiary amine groups may be formed after modification reaction; and (3) the mannosamine on the surface of HPAMAM may alter the periphery structure of the hyperbranched macromolecules leading to strong fluorescence.<sup>30</sup> Therefore, the surface modification of the resultant HPAMAMs was carried out by Michael addition reaction of mannosamine with acrylate groups. This reaction is very efficient when the acrylate group reacts with the primary amine under mild conditions.<sup>31</sup> Thus, the first step is the synthesis of HPAMAMs with the acrylate groups on their surface. In the Michael addition polymerization of A2 + B3 monomers, the surface group of the resultant HPAMAMs is determined by the ratio of two monomers.<sup>31–33</sup> The polymerization with a feed molar ratio (2/1) of the diacrylate to triamine compounds yielded the HPAMAMs with surface acrylate groups.<sup>31</sup> Therefore, the acrylate-functionalized HPAMAMs were prepared by Michael addition polymerization of CBA and AEPZ with a molar ratio of 2:1, and their structure was characterized by its <sup>13</sup>C NMR spectra. In Figure 1A, we can see the characteristic vinyl carbon signals at  $\delta = 126$  (1) and 132 ppm (2), indicating the existence of acrylate groups on the surface of HPAMAMs. The two carbon signals of the three methylene groups next to the tertiary amine at  $\delta = 50$  (g) and 50.5 ppm (i) are ascribed to transformation of the secondary amine (formed) into a tertiary amine forming branched structure, and the ascription of other carbons in HPAMAMs is marked in Figure 1B. The hyperbranched structure was also confirmed by its <sup>1</sup>H NMR spectrum in Figure

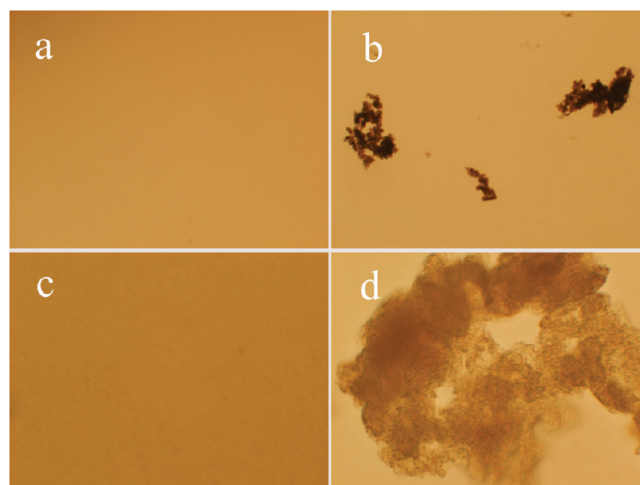


**Figure 9.** Phase contrast images of (a) *E. coli* cells at OD1.0 ( $\times 4$ ); (b) Aggregates of *E. coli*/M-HPAMAMs solution ( $\times 4$ ); (c) *E. coli* cells at OD1.0 ( $\times 40$ ); (d) Aggregates of *E. coli*/M-HPAMAMs solution ( $\times 40$ ).

2A. The vinyl protons of the acrylate groups are at  $\delta = 6.17$ , 6.08, and 5.58 ppm, and other signals are marked in this figure. These results are the same with our previous studies.<sup>31,34</sup>

The molecular weights of the HPAMAMs obtained at different polymerization times were measured by GPC, and the results are shown in Figure 3. With the evolution of polymerization, the molecular weights of resulting HPAMAMs increased slowly at the initial polymerization and then increased fast at the last stage of polymerization, while the molecular weight distribution became broad. These are the general phenomena in the hyperbranched polymerization. The HPAMAM with  $M_n = 17500$ ;  $M_w/M_n = 1.42$  was used in the following studies except where specially mentioned.

In our previous study, we found that the acrylate groups reacted readily with primary amine via Michael addition reaction.<sup>31</sup> Therefore, the reaction of acrylate-functionalized HPAMAMs with D-mannosamine was carried out. After purified by precipitation, the mannose-functionalized HPAMAMs (M-HPAMAMs) was obtained. For verifying the mannose groups on the surface of HPAMAMs, the <sup>1</sup>H NMR spectra were measured. A typical <sup>1</sup>H NMR spectrum in Figure 2B demonstrates the characteristic proton signals of the mannose at  $\delta = 5.13$ , 3.98, 3.82, and 3.21 ppm. Thus, the mannose-functionalized HPAMAMs (M-HPAMAMs) were successfully prepared. But the proton signals of the residual acrylate groups at  $\delta = 5.75$  and  $\sim 6.15$  ppm can be seen clearly, indicating that the complete substitution of vinyl groups was not achieved probably

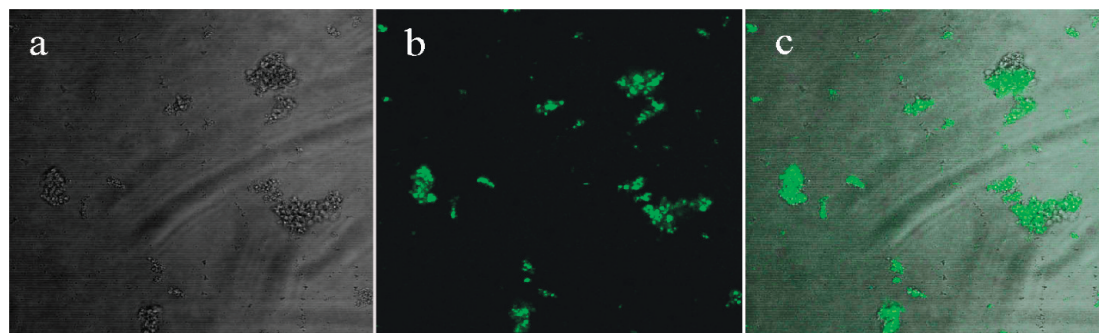


**Figure 10.** Laser scanning confocal microscopy images of *E. coli* (OD 1.0)/M-HPAMAS aggregates in PBS solution: (a) bright field, (b) excited wavelength at 488 nm, (c) merging of photos a and b.

due to high steric hindrance of mannosamine ring. But this benefits further reaction of the acrylate with the secondary amine (formed), producing the tertiary amine groups.

**Fluorescent Properties of M-HPAMAMs.** To acquire the HPAMAMs with fluorescence strong enough in various applications, we studied the effects of molecular weight and surface modification of the resulting HPAMAMs on the photoluminescence. Under excitation at 370 nm, the HPAMAMs with surface acrylate groups in aqueous solution (pH = 7.0) with concentration of 1 mg/mL displayed two fluorescent bands at 430 and  $\sim$ 459 nm, respectively (Figure 4), and the former may be related to the surface acrylate groups because the fluorescence at 430 nm disappeared completely after treatment with mannosamine (Figure 5). With an increase in the molecular weights from 8600 to 17200 g/mol, the fluorescence at  $\sim$ 459 nm enhanced significantly, but the intensity at 430 nm was relatively less increased, so the former increased obviously and the latter decreased relatively. When the molecular weights increased from 11600 to 17200 g/mol, we can see obvious red-shift of the fluorescence from  $\sim$ 459 to 468 nm (Figure 4). This might be due to the relative increase in the tertiary amino units and the more rigid and crowded periphery of the high molecular weight HPAMAMs. However, only by enhancing molecular weights of HPAMAMs, the fluorescence of the resulting HPAMAMs was still weak. As aforementioned, surface modification may be a more efficient strategy to enhance the fluorescence. D-Mannosamine was used to modify the surface of the HPAMAMs via Michael addition reaction. The fluorescence properties of the HPAMAMs before and after surface modification were measured, and the results are shown in Figure 5. We can see that the M-HPAMAMs with  $M_n = 17200$  g/mol emitted a much stronger fluorescence ( $\sim$ 340 times) than its precursor. Probably, the D-mannose is an optical compound and has a ring as well as four hydroxyl groups, and these may restrict rotational motion of the terminal chains in the periphery of HPAMAMs.<sup>30</sup> This will decrease collisional relaxation and self-quenching.

In studying the fluorescence properties of M-HPAMAMs, we observed an interesting phenomenon, the fluorescent spectra of M-HPAMAMs are quite broad, depending on excitation wavelengths (Figure 6). The M-HPAMAMs emitted multicolor fluorescence when excited by any wavelength from 340 to 520 nm. This is different from the organic fluorophores.<sup>35</sup> Figure 6 shows that the solution of M-HPAMAMs in water was excited at from 340 nm to 520 nm with 20 nm increment, respectively, strong fluorescence appeared at different wavelength. This phenomenon was highly reproducible. The hyperbranched polymers possess a three-dimensional branched structure, their molecular weight distributions are quite broad, and the structures in the periphery of M-HPAMAMs become more compact with

increase of molecular weights. This may be the reason for the broad fluorescent spectrum.

**Interaction of *Escherichia coli* (*E. coli*) with M-HPAMAMs.** To test whether the M-HPAMAMs can be used in detection of the bacteria, *Escherichia coli* (*E. coli*) BL21, which is a normal inhabitant of the intestine,<sup>36</sup> was used in this study. After incubating 4 mL of *E. coli* suspension at an OD600 of 1.0 with 50  $\mu$ L of PBS solution of the fluorescent M-HPAMAMs (10 mg/mL) for 30 min, lots of clusters, which might be formed from congregation of the aggregates of bacteria linked by the M-HPAMAMs (Figure 7). To verify this presumption, we collected the precipitates by centrifugation of the suspension. The precipitates obtained were washed with PBS solution three times for complete removal of the unbound M-HPAMAMs and then were resuspended in 4 mL of PBS solution. A sample was taken from the resuspended solution for observation under a laser confocal fluorescence microscope. The blue, green, and red precipitates were observed when excited at wavelengths of 800 (dual-photo excitation), 480 and 543 nm, respectively (Figure 8). This demonstrates that the M-HPAMAMs have strong affinity with the bacteria because *E. coli* can not; only the M-HPAMAMs can emit colorful fluorescence upon different excitation wavelengths.

To further clarify the precipitates, the phase contrast microscope was used to observe the precipitates. We can see several big clusters in Figure 9b, and the detailed structures of clusters are shown in Figure 9d. These might be the result of many bacteria that are bound by M-HPAMAMs, because no cluster was observed for the bacteria in PBS solution (Figure 9a,c) or for the M-HPAMAMs in solution (the images are not shown). A photo of the clusters in Figure 9d displays a tinged area between many dark strips, which may be ascribed to a connection of several bacteria by the M-HPAMAMs forming aggregates. So, the big clusters are probably formed by the flocculation of many aggregates. The mannose-binding bacteria can be seen clearly in Figure 10a–c. In the photo of laser scanning confocal microscopy for the precipitates under a bright field, we can see that the big clusters are composed of many particles (Figure 10a), which are ascribed to the aggregates of bacteria because the unbound M-HPAMAMs were washed out. Under excitation at 488 nm, the big clusters emitted bright fluorescence (Figure 10b,c). Because *E. coli* can not emit fluorescence, the bright fluorescence might be from the M-HPAMAMs in the clusters. Therefore, the connection of bacteria by M-HPAMAMs was taken place when the polymer solution was added to the PBS solution of *E. coli* cells. The TEM image of *E. coli* displays well-dispersion of individual bacterium (Figure 11a), but the TEM image of *E. coli*/M-HPAMAMs in Figure 11b shows big aggregates. This must be a result of the connection of the bacteria with M-HPAMAMs.

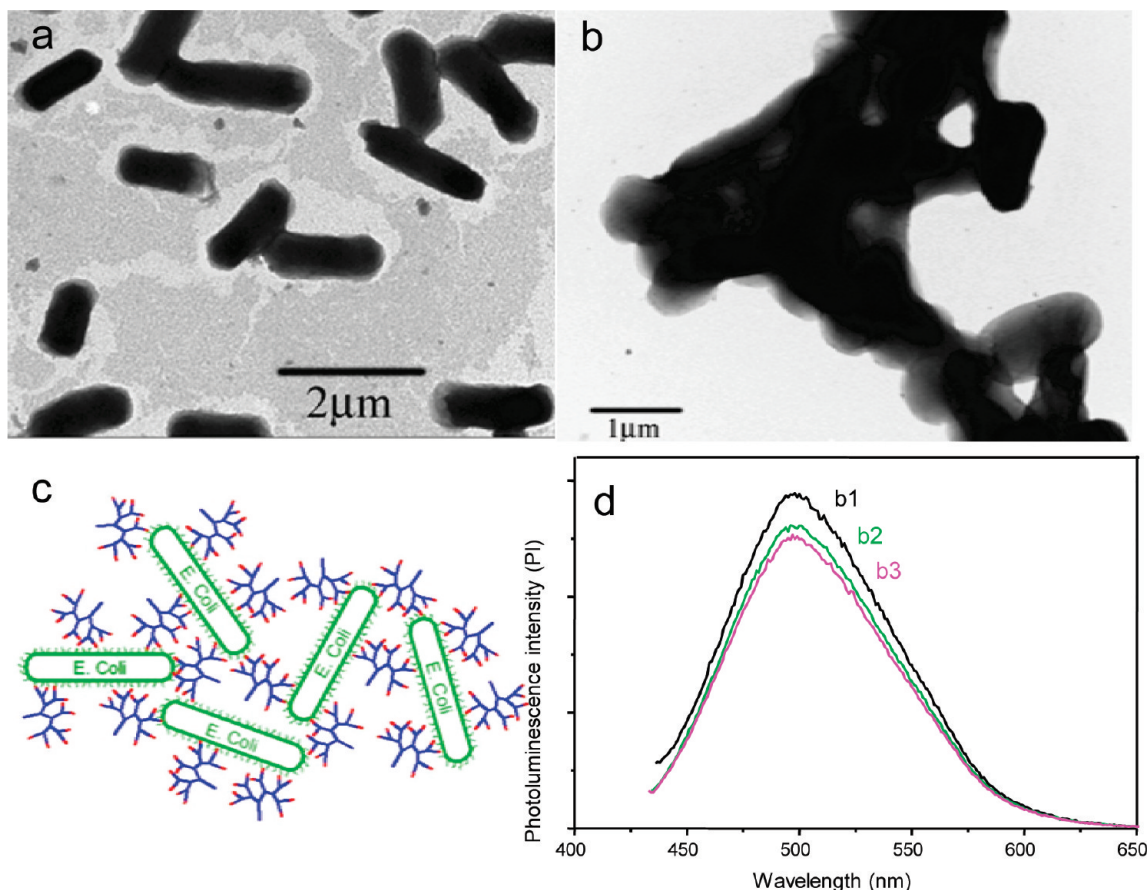


**Figure 11.** TEM images of *E. coli* (a) and *E. coli*/M-HPAMAMs aggregates (b; scale bar: a, 2  $\mu\text{m}$ ; b, 1  $\mu\text{m}$ ; 1% phosphotungstic acid was used to negatively stain *E. coli*/M-HPAMAMs aggregates); Schematic representation for formation of the M-HPAMAMs/*E. coli* aggregation (c); Fluorescent spectra of M-HPAMAMs solution in the absence (b1) and in the presence of different *E. coli* concentrations; b2,  $10^6$ ; b3,  $10^7$  cfu/mL;  $\lambda_{\text{ex}} = 420$  nm; polymer concentration, 0.125 mg/mL (d).

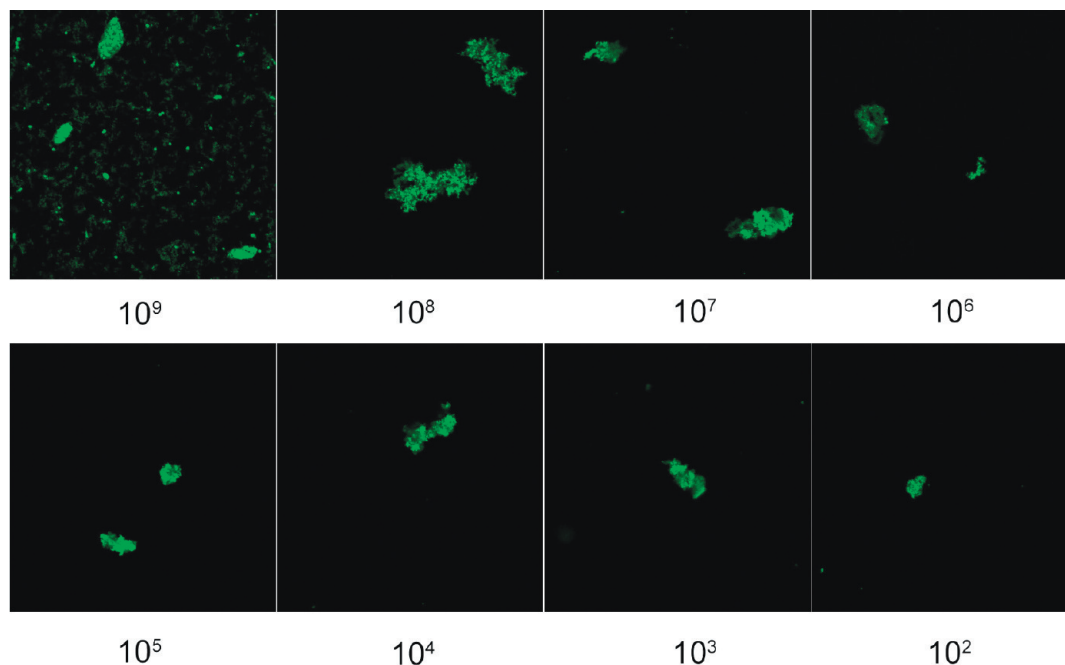


**Figure 12.** Detection limit for the staining of the mannose-binding *E. coli* by M-HPAMAMs, and the number of bacteria incubated with the polymer-containing solution is indicated below each image.

As we mentioned, the M-HPAMAMs have numerous surface mannose groups, every macromolecule can interact with several bacteria, so its function is similar to a cross-linker of the clusters.

Many bacteria were bound by M-HPAMAMs macromolecules to form aggregates; their further aggregation produced the clusters, as shown in Figure 11c. We observed the linear



relationship of fluorescent intensity with Con A concentration (data is not shown), but such a property was difficult to be obtained, probably due to the light scattering effect of particles. After the solution was centrifuged, the fluorescent intensity of the upper clean solution decreased with increase of the *E. coli* concentration (Figure 11d). When the concentration of *E. coli* was high, mixing of M-HPAMAM with *E. coli* solution yielded precipitates (Figure 7). Fluorescence of the resultant solution measured after removal of the cluster by centrifugation decreased due to a concentration decrease of the M-HPAMAMs in solution.

According to the method reported previously,<sup>24</sup> the detection limit was determined. A series of *E. coli* concentrations in PBS solution ( $10^9 \sim 10^2$  cfu/mL) were prepared through continuous dilution, and then the resultant solutions were incubated with M-HPAMAMs. After removal of the unbound polymer in the precipitates via washing thoroughly with PBS solution, the fluorescence microscopy of the resulting precipitates was used to determine the detection limit. Results in Figure 12 show that fluorescent aggregates of the bacteria can be observed until concentration of  $10^2$  cfu/mL. This detection limit is much lower than that ( $10^4$  cfu/mL) of the fluorescent conjugated polymers.<sup>24</sup> When the concentration of bacteria was lower than  $10^2$  cfu/mL, no fluorescent aggregates was observed. Furthermore, the number and size of the fluorescent clusters decreased with diminishing bacteria numbers as shown in Figure 12.

## Conclusions

Biocompatible mannose-functionalized HPAMAMs have been successfully prepared via Michael addition polymerization and successively surface modified with mannosamine in one-pot. The resulting M-HPAMAM can emit strong and multicolor fluorescence depending upon the excitation wavelengths, and the photoluminescence of M-HPAMAMs is much stronger (340 times) than that of their precursors. The mannose groups on the surface of M-HPAMAM have a strong affinity to bacteria, and incubation of the M-HPAMAMs with *E. coli* yields brightly fluorescent bacteria clusters due to polyvalent interactions between M-HPAMAMs and *E. coli*. The fluorescent intensity of the residual aqueous solution lowered. The detection limitation of this method is  $10^2$  cfu/mL. This new type of fluorescence material has potential applications in cell imaging, biosensing, and drug delivery.

**Acknowledgment.** We thank the National Natural Science Foundation of China for financial support under Contract Nos. 50673086 and 50633010.

## References and Notes

- (1) Ferruti, P.; Marchisio, M. A.; Duncan, R. *Macromol. Rapid Commun.* **2002**, *23*, 332–355.
- (2) Wu, D. C.; Liu, Y.; Jiang, X.; Chen, L.; He, C. B.; Goh, S. H.; Leong, K. W. *Biomacromolecules* **2005**, *6*, 3166–3173.
- (3) Lin, C.; Zhong, Z.; Lok, M. C.; Jiang, X.; Hennink, W. E.; Feijen, J.; Engbersen, J. F. J. *Bioconjugate Chem.* **2007**, *18* (1), 138–145.
- (4) Lin, C.; Zhong, Z.; Lok, M. C.; Jiang, X.; Hennink, W. E.; Feijen, J.; Engbersen, J. F. J. *J. Controlled Release* **2006**, *116* (2), 130–137.
- (5) Esfand, R.; Tomalia, D. A. *Drug Discovery Today* **2001**, *6*, 427–436.
- (6) Blacklock, J.; You, Y. Z.; Zhou, Q. H.; Mao, G. Z.; Oupick, D. *Biomaterials* **2009**, *30*, 939–950.
- (7) Wu, D. C.; Liu, Y.; Jiang, X.; He, C. B.; Goh, S. H.; Leong, K. W. *Biomacromolecules* **2006**, *7*, 1879–1883.
- (8) Chew, S. A.; Hacker, M. C.; Saraf, A.; Raphael, R. M.; Kasper, F. K.; Mikos, A. G. *Biomacromolecules* **2009**, *10*, 2436–2445.
- (9) Kono, K.; Kojima, C.; Hayashi, N.; Nishisaka, E.; Kiura, K.; Watarai, S.; Harada, A. *Biomaterials* **2008**, *29*, 1664–1675.
- (10) Perumal, O. P.; Inapagolla, R.; Kannan, S.; Kannan, R. M. *Biomaterials* **2008**, *29*, 3469–3476.
- (11) Wu, D. C.; Liu, Y.; He, C. B. *Macromolecules* **2008**, *41*, 18–20.
- (12) Yang, W.; Pan, C. Y. *Macromol. Rapid Commun.* **2009**, *30*, 2096–2101.
- (13) Wang, D.; Imae, T. *J. Am. Chem. Soc.* **2004**, *126*, 13204–13205.
- (14) Wu, D.; Liu, Y.; He, C.; Goh, S. H. *Macromolecules* **2005**, *38*, 9906–9909.
- (15) Freeman, C. G.; McEwan, M. J.; Claridge, R. F. C.; Phillips, L. F. *Chem. Phys. Lett.* **1971**, *8*, 77–78.
- (16) Newman, R. H.; Freeman, C. G.; McEwan, M. J.; Claridge, R. F. C.; Phillips, L. E. *Trans. Faraday Soc.* **1971**, *67*, 1360–1364.
- (17) Bettelheim, K. A.; Beutin, L. J. *J. Appl. Microbiol.* **2003**, *95*, 205–217.
- (18) Yu, L. S. L.; Reed, S. A.; Golden, M. H. *J. Microbiol. Methods* **2002**, *49*, 63–68.
- (19) Zhao, X. J.; Hilliard, L. R.; Mechery, S. J.; Wang, Y. P.; Bagwe, R. P.; Jin, S. G.; Tan, W. H. *Proc. Natl. Acad. Sci. U.S.A.* **2004**, *101*, 15027–15032.
- (20) Phillips, R. L.; Miranda, O. R.; You, C. C. *Angew. Chem., Int. Ed.* **2008**, *47*, 2590–2594.
- (21) El-Boubbou, K.; Gruden, C.; Huang, X. *J. Am. Chem. Soc.* **2007**, *129*, 13392–13393.
- (22) Gao, J.; Li, L.; Ho, P.-L.; Mak, G. C.; Gu, H. W.; Xu, B. *Adv. Mater.* **2006**, *18*, 3145–3148.
- (23) Disney, M. D.; Zheng, J.; Swager, T. M.; Seeberger, P. H. *J. Am. Chem. Soc.* **2004**, *126*, 13343–13346.
- (24) Paulson, J. C.; Blixt, O.; Collins, B. E. *Nat. Chem. Biol.* **2006**, *2*, 238–248.
- (25) Xue, C. H.; Jog, S. P.; Murthy, P.; Liu, H. Y. *Biomacromolecules* **2006**, *7*, 2470–2474.
- (26) Müller, M. K.; Brunsveld, L. *Angew. Chem., Int. Ed.* **2009**, *48*, 2921–2924.
- (27) Yang, J.; Zhang, Y.; Gautam, S.; Liuc, L.; Dey, J.; Chen, W.; Mason, R. P.; Serrano, C. A.; Schuge, K. A.; Tang, L. *Proc. Natl. Acad. Sci. U.S.A.* **2009**, *106*, 10086–10091.
- (28) Gross, R. A.; Kalra, B. *Science* **2002**, *97*, 803–807.
- (29) Oh, J. K.; Siegwart, D. J.; Lee, H.; Sherwood, G.; Peteanu, L.; Hollinger, J. O.; Kataoka, K.; Matyjaszewski, K. *J. Am. Chem. Soc.* **2007**, *129*, 5939–5945.
- (30) Chu, C.-C.; Imae, T. *Macromol. Rapid Commun.* **2009**, *30*, 89–93.
- (31) Wang, D.; Liu, Y.; Hong, C. Y.; Pan, C. Y. *J. Polym. Sci., Part A: Polym. Chem.* **2005**, *43*, 5127–5137.
- (32) Hong, C. Y.; You, Y. Z.; Wu, D.; Liu, Y.; Pan, C. Y. *J. Am. Chem. Soc.* **2007**, *129*, 5354–5355.
- (33) Wang, H. B.; Chen, X. S.; Pan, C. Y. *Eur. Polym. J.* **2008**, *44*, 2184–2193.
- (34) You, Y. Z.; Hong, C. Y.; Pan, C. Y. *Macromolecules* **2009**, *42*, 573–575.
- (35) Jaiswal, J. K.; Mattoussi, H.; Mauro, J. M.; Simon, S. M. *Nat. Biotechnol.* **2003**, *21*, 47–51.
- (36) Kalele, S. A.; Kundu, A. A.; Gosavi, S. W.; Deobagkar, D. N.; Deobagkar, D. D.; Kulkarni, S. K. *Small* **2006**, *2*, 335–338.

BM100307D